Materials Science & Engineering A 646 (2015) 45–51

Contents lists available at ScienceDirect

Materials Science & Engineering A

journal homepage: www.elsevier.com/locate/msea

Microstructural stability and tensile properties of a Ti-containing single-crystal Co–Ni–Al–W-base alloy

L. Shi, J.J. Yu*, C.Y. Cui, X.F. Sun

Institute of Metal Research, Chinese Academy of Sciences, 72 Wenhua Road, Shenyang 110016, China

ARTICLE INFO

Article history:
Received 29 June 2015
Received in revised form
14 August 2015
Accepted 14 August 2015
Available online 15 August 2015

Keywords:
Co–Al–W-base alloy
Microstructures
Tensile properties
Dislocation structures

ABSTRACT

Microstructural stability and tensile properties of a Ti-containing single-crystal Co–Ni–Al–W-alloy with low tungsten content have been investigated. The alloy possesses relatively lower density and higher γ′ solvus temperature compared to some high-tungsten-content Co–Al–W-base alloys. After aging at 900–1000 °C for 400 h, the alloy maintains the stable γ/γ′ two-phase microstructure without the presence of secondary phases. In the low and medium temperature range (R.T.–800 °C), the alloy exhibits superior tensile strength compared to the reported single-crystal Co–Al–W-base alloys, while above 800 °C, the yield stress decreases rapidly with temperature increasing. The major deformation mechanisms of the alloy consist of shearing of the γ′ precipitates by pairs of $a/2\langle 110\rangle$-type dislocations from room temperature to 800 °C and bypassing of the γ′ precipitates by $a/2\langle 110\rangle$-type matrix dislocations above 900 °C. At 900 °C, it shows a transition from the γ′ shearing to bypassing.

1. Introduction

Compared to conventional Co-base superalloys which are mainly dependent on the solid solution hardening and carbide strengthening, Ni-base superalloys possess more outstanding mechanical properties because of the well known strengthening of $L1_2$ type γ′ (Ni_3Al) precipitates [1]. The discovery of a relatively stable γ′-Co_3 (Al,W) phase with $L1_2$ structure in the ternary Co–Al–W system by Sato et al. [2] provides a possibility to develop a new class of γ′-strengthened Co-base superalloys. The primary researches on the physical and mechanical properties of Co–Al–W-base alloys indicate that the γ′-Co_3 (Al,W) can be practically used as the strengthening phase [2–16].

In an attempt to further improve the γ′-Co_3 (Al,W) phase stability and mechanical properties of Co–Al–W-base alloys, various alloying elements have been investigated. Among those elements, Ti and Ta are of special interest as they are known to increase the γ′-Co_3 (Al,W) solvus temperature and high-temperature strength [3–16]. Adding about 2 at% Ti to the Co–9Al–9W (at%) raises the γ′-Co_3 (Al,W) solvus temperature about 110 °C [3]. The addition of Ti can increase the γ+γ′ two-phase field, while an exceedingly high amount of Ti promotes the formation of the deleterious phase Co_2AlTi [4,5]. In the ternary Co–Al–W system [7], with a 2 at% Ta addition, the γ′ solvus temperature is increased by 79 °C and the yield strength at 800 °C is increased from 360 to 580 MPa. The results from Xue et al. [8] show that the γ′ solvus temperature, γ′ volume fraction and creep strength are increased significantly by additions of Ta and Ti in a ternary Co–Al–W system. First-principles calculations suggest that additions of Ti and Ta to the Al or W atomic sites can increase the superlattice intrinsic stacking fault (SISF) energy of the stoichiometric Co_3 (Al,W) compound [9]. The increment of SISF energy affects the high-temperature deformation behaviors [7,8,10], which may be responsible for the improved high-temperature mechanical properties in the Ta- and Ti-containing Co–Al–W-base alloys [7,8,10].

However, in these studies [3,6–10], the amount of W or (W+Ta) is over 8 at%, much larger than that of Ni-base superalloys. Thus, these alloys have a much higher density ($>9.3\ g\ cm^{-3}$) compared to Ni-base superalloys, restricting the application in turbine blades for aero engines. The investigations by Shinagawa et al. [11] suggest that the γ′-Co_3 (Al,W) continuously exists from the Co side to the Ni side in the Co–Ni–Al–W system and the γ+γ′ two-phase field widens to the low W region with increasing Ni content. There is a possibility that substitution of Ni for partial W and alloying lighter elements such as Ti can stabilize the γ′ phase at high temperature. Therefore, in the present study, we aim to explore the microstructural stability and tensile properties of a Co–Ni–Al–W–Ti alloy with a low amount of tungsten.

2. Experimental procedure

The nominal composition (at%) of the alloy studied in this work is as follows: Al 9, W 5, Ni 17, Ti 3, balance by Co (named as 3Ti).

* Corresponding author.
E-mail address: jjyu@imr.ac.cn (J.J. Yu).

http://dx.doi.org/10.1016/j.msea.2015.08.044
0921-5093/

The master alloy was melted in a vacuum induction furnace, and then directionally solidified into [001] single crystal rods by Bridgman technique at a constant withdraw rate of 6 mm/min. The melting point and the γ′ solvus temperature were determined by Differential Thermal Analysis (DTA) under high purity Ar atmosphere with a heating rate of 10 °C/min. Crystal orientations of single-crystal bars were determined by electron backscatter diffraction (EBSD) analysis technology and specimens with deviation from [001] within 10° were used. Samples were placed in quartz tubes back-filled with Ar gas before heat treatments. The standard heat treatment (SHT) was carried out as follows: 1250 °C /12 h, furnace cooling+950 °C/84 h, air cooling+750 °C/24 h, air cooling. Additional long term aging treatment at 900, 950 and 1000 °C for 400 h was utilized to evaluate the microstructural stability after SHT. Heat-treated samples were polished in a solution of 42 ml H_3PO_4 +34 ml H_2SO_4+ 24 ml H_2O at 10 V. The microstructure was analyzed using a Scanning Electron Microscope (SEM). The volume fraction and size of the γ′ precipitates were analyzed by the image analyzer. The equilibrium compositions of the γ′ and γ phases at 1000 °C were determined by electron probe microanalysis (EPMA).

Tensile specimens with a nominal 25 mm gage length and a diameter of 3 mm were machined from samples after SHT. Tensile tests were conducted at a strain rate of $1\times10^{-4}\,s^{-1}$ from room temperature to 1000 °C with the crystal growth direction parallel to the tension loading direction. During the tests, the temperature variation was maintained within ± 2 °C. At least two identical specimens were tested at each temperature. Transverse sections of the deformed specimens were cut into disks with 0.5 mm in thickness. These disks were polished to 50 μm, and then subjected to twin-jet polishing in a solution of methanol with 5 vol% perchloric acid at −30 °C and 18–20 V. A JEM 2100 Transmission Electron Microscope (TEM) was used for dislocation analysis.

3. Results

3.1. The γ′-Co_3 (AL,W) solvus temperature

The transformation temperatures measured by DTA are given in Table 1. For comparison, the transformation temperatures of other Co-base superalloys with γ/γ′ microstructure are also given in Table 1. It can be seen that the γ′ solvus temperature decreases greatly when the W content is reduced from 9 at% to 6.8 at%, suggesting that high amount of W is beneficial to improve the high-temperature stability of the γ′-Co_3 (Al,W) in the ternary Co–Al–W systems. By comparing the Co–7.3Al–6.8W (at%) and the Co–7.3Al–7.2W–20.2Ni (at%), the γ′ solvus temperature increases slightly with Ni additions. Adding Ti to the ternary Co–Al–W systems can increase the γ′ solvus temperature markedly. The 3Ti alloy exhibits the γ′ solvus temperature 10 °C higher than the Co–7Al–8W–4Ti (at%). Moreover, the γ′ solvus temperature of the 3Ti alloy and the Co–8.8Al–9.8W–2Ta (at%) is approaching. These results indicate that a combined addition of Ti and Ni is effective to improve the γ′ solvus temperature. As shown in Table 1, the 3Ti alloy has a density of 8.87 g cm^{-3}, which is close to the level of single-crystal Ni-base superalloys. Therefore, it is feasible to lower the density by substituting partial W with Ni and alloying lighter elements such as Ti whilst still possessing a sufficiently high γ′ solvus temperature.

Table 1
Liquidus, solidus, γ′-solvus temperatures and density of the 3Ti alloy, together with those of other Co–Al–W-base alloys.

Alloy	Transformation temperature (°C)			Density (g cm^{-3})
	Solidus	Liquidus	γ′ solvus	
3Ti	1369	1424	1080	8.87
Co–7.3Al–6.8W (at%) [12]	–	–	854	9.18
Co–9.2Al–9W (at%) [3]	1441	1466	985	9.54
Co–7.3Al–7.2W–20.2Ni (at%) [12]	–	–	881	9.29
Co–6.4Al–6.0W–2.2Ti (at%) [12]	–	–	983	9.09
Co–7Al–8W–4Ti [8]	–	–	1070	–
Co–8.8Al–9.8W–2Ta (at%) [7]	1407	1451	1079	> 9.54

3.2. Microstructural stability and partition behavior of alloying elements between the γ and γ′ phases

Fig. 1 shows the typical microstructure of the 3Ti alloy after aging at 900–1000 °C for 400 h. It is obvious that the morphology of the γ′ particles is nearly cubic, aligning along a certain direction. With the increase of annealing temperature, the volume fraction of the γ′ precipitates decreases, which probably results from a higher solute supersaturation at lower annealing temperature of 900 °C as compared to that of 1000 °C. In some Ti-containing Co–Al–W-base alloys [4,5,13], the β-Co_2AlTi phase appears after annealing at high temperature. This kind of phase is considered as a deleterious phase, which is not coherent with the γ matrix and deteriorates the high-temperature properties. The 3Ti alloy exhibits the γ–γ′ microstructure without the presence of secondary phases, suggesting that substituting partial W with Ni and alloying Ti are beneficial to improve microstructural stability at high temperature.

Fig. 2 shows TEM images of the 3Ti alloy after SHT. The cuboidal γ′ precipitates are coherent with the matrix. The average size of the γ′ precipitates is about 0.5 μm and the γ′ volume fraction is about 70%. Isolated dislocations are occasionally observed at the interfaces, and a few matrix dislocations are bowed through the γ matrix channels. Furthermore, there are several dislocations which appear to have taken a 90° change in direction during the process of traveling through the γ matrix (Fig. 2c).

The size of the γ and γ′ phases in the specimens that were annealed at 1000 °C for 400 h is larger than 1 μm in some regions, which is available for quantitative analysis of the two phases by using EPMA. The phase compositions and partition coefficient $K_{\gamma'/\gamma}$ ($=C_{\gamma'}/C_{\gamma}$) of each element at 1000 °C are listed in Table 2, where $C_{\gamma'}$ and C_{γ} are equilibrium compositions of elements in the γ′ and γ phases. As shown in Table 2, Al and Ni slightly partition to the γ′ phase, while W and Ti show a bit stronger partitioning tendency to the γ′ phase. The sum of the Al (~9.9 at%), W (~5.27 at%) and Ti (~4.44 at%) contents in the γ′ phase is 19.61 at%, less than the stoichiometric value of 25 at%. Similar results are found in a Ni-containing Co–Al–W-base alloy [14]. The nominal stoichiometry of the γ′ phase in the Co–8Al–8W–25Ni (at%) is inferred as $(Co, Ni)_3(Al, W, Ni)$ [14], suggesting that Ni atoms occupy both Co sites and Al/W sites. It is confirmed by atom probe tomography (APT) that Ti atoms occupy the Al/W sites [15]. It is likely that some Ni atoms may have also substituted on the Al/W sites in the present alloy. Therefore, the nominal stoichiometry of the γ′ phase in the present study can be deduced as $(Co, Ni)_3(Al, W, Ni, Ti)$.

3.3. Temperature dependence of the 0.2% yield stress

The 0.2% yield strength as a function of temperature is plotted in Fig.3. For comparison, three γ′-strengthened single-crystal Co-base alloys [7,16] are also included. Similar to other Co-base alloys in Fig. 3, the 3Ti alloy exhibits a three-stage temperature dependence of the stress. In the low temperature range (below 600 °C), the yield strength decreases with the increase of temperature. In

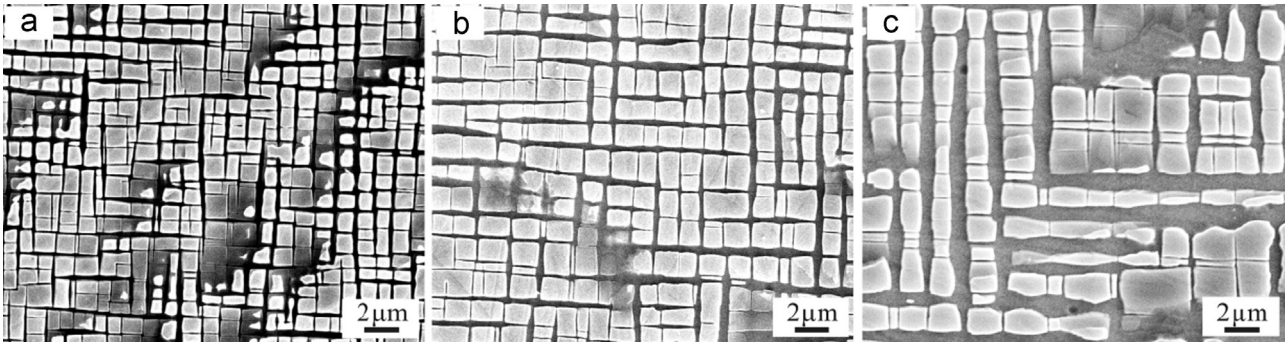

Fig. 1. Typical SEM microstructures of the 3Ti alloy after long-term aging: (a) 900 °C, (b) 950 °C and (c) 1000 °C for 400 h.

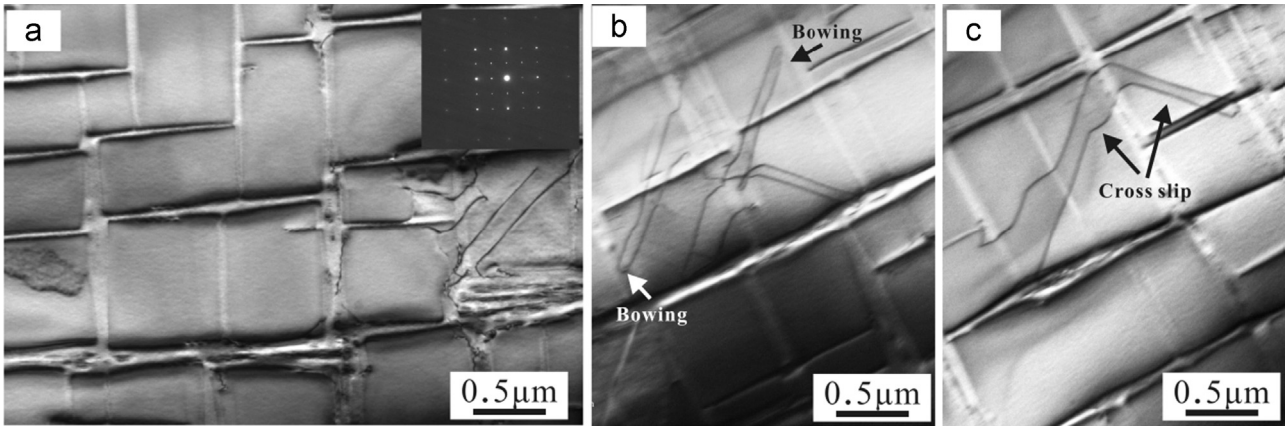

Fig. 2. Bright-field TEM images of the 3Ti alloy after SHT (a). The bowing (b) and cross slip (c) of dislocations in the γ matrix can be observed. Images are taken with beam direction [001].

Table 2
Equilibrium compositions of the 3Ti alloy at 1000 °C (at%) and partition coefficient $K_{\gamma'/\gamma}$ of each element.

Position	Co	Al	W	Ni	Ti
γ′	62.18 ± 0.53	9.90 ± 0.25	5.27 ± 0.34	18.19 ± 0.41	4.44 ± 0.27
γ	69.38 ± 0.63	8.70 ± 0.35	3.34 ± 0.61	15.87 ± 0.29	2.67 ± 0.19
Coefficient ($K_{\gamma'/\gamma}$)	0.90	1.14	1.58	1.15	1.66

intermediate temperature range an anomalous behavior is found which peaks at around 800 °C. In the high temperature range (above 800 °C), the strength decreases again. From room temperature to 800 °C, the yield strength of the 3Ti alloy is higher compared to other Co–Al–W-base alloys shown in Fig.3. Above 800 °C, the 3Ti alloy exhibits a rapid decrease in the yield stress. At 1000 °C, the 0.2% yield stress of the 3Ti alloy is about 100 MPa lower than that of the Co–10Al–5W–17Ni–6Cr–2.7Ta (at%). This result suggests that the addition of Ti is beneficial to improve the low and medium temperature strength.

3.4. Dislocation structures

3.4.1. Low and medium temperature range (R.T.–800 °C)

Fig. 4 demonstrates the deformation microstructures after deformation at room temperature. Stacking faults (SFs) can be frequently observed in the γ channels. In a Ta-containing Co–Al–W-base alloy [16], SFs appear in the γ channels after tensile testing at room temperature. The disassociation of a matrix dislocation in channels can be favored by a decrease in the matrix SF energy [17]. It is generally believed that the SF energy of the γ (Co) matrix is low. Therefore, the formation of SFs in the γ channels is due to its low SF energy. Pairs of $a/2\langle 110\rangle$-type dislocations in the γ′ precipitates can be observed (marked by black arrows), indicating the shearing mechanism.

The deformation microstructure of the 3Ti alloy at 600 °C is shown in Fig. 5. Similar with the observations at room temperature, pairs of $a/2\langle 110\rangle$-type dislocations shearing the γ′ precipitates are observed as well. The fault loop within the γ′ precipitates is occasionally observed (Fig. 5b). SFs in the γ channels can be occasionally observed as well. From the consideration of phase stability, the SF energy of the γ (Co) matrix is expected to increase with temperature because the matrix with fcc structure in Co-base alloys is more stable at high temperature, and the matrix with hcp structure is more stable at low temperature. The positive correlation between the SF energy and temperature results in the occasional observation of SFs after high temperature deformation.

Dislocation configurations at 700 °C are demonstrated in Fig. 6. Some dislocations are shearing the γ′ precipitates (marked by black arrow). SFs in the γ channels are scarcely observed.

For the specimens deformed at 600 °C and 700 °C, in some regions, a special dislocation microstructure is observed, as demonstrated in Fig. 7. In these regions, dislocations cross each other and form 90° angles. Similar dislocation microstructures were reported in a ternary Co–Al–W-base alloy crept at 850 °C/450 MPa [18] as well as in a single-crystal Ni-base superalloy under 760 °C/

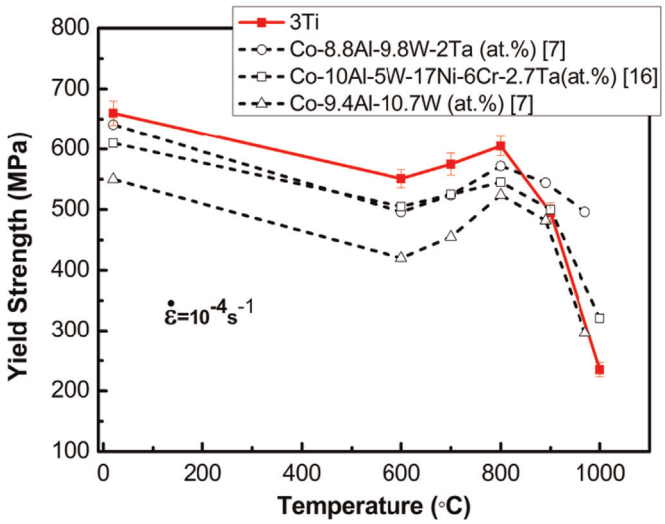

Fig. 3. Temperature dependence of the 0.2% yield strength of the 3Ti alloy: together with 0.2% yield stresses of three single-crystal γ/γ′ two-phase Co-base alloys.

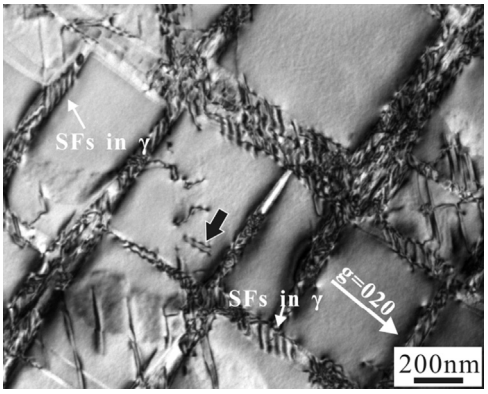

Fig. 4. Bright-field TEM image of the 3Ti alloy deformed in tension at room temperature to 5%. Beam direction close to the [001] zone axial using a (020) reflection.

840 MPa [19]. It is interesting to note that such dislocation microstructure occurred at a relatively lower temperature and higher stress (a bit higher than yield stress) conditions in the present alloy. The initial dislocation microstructures can affect the dislocation motion during subsequent creep deformation [20]. In CMSX-3, networks of dislocations contained in the matrix are occasionally observed in the aged samples [20]. In the initial creep stage, dislocations spread from these areas into the previously dislocation free areas and some dislocations take a 90° change in direction during the process of traveling through the matrix [20]. These observations suggest that dislocation networks formed during heat treatments can serve as sources that promote the spreading and cross slip of dislocations in the matrix. Tensile tests are a transient deformation process, analogous to the deformation behavior in the initial creep stage. As shown in Fig.2, the bowing and cross slip of dislocations are observed in some regions. These regions may play a similar role as the networks reported in Ref. [20]. During tension, dislocation spreading in the matrix is activated in these regions and dislocation cross-slip occurs due to the cross gliding of the leading screw dislocation segments from two different {111} slip planes [20]. Dislocations with same burgers vector operating on two {111} planes can form the pattern of dislocation lines intersecting under 90°.

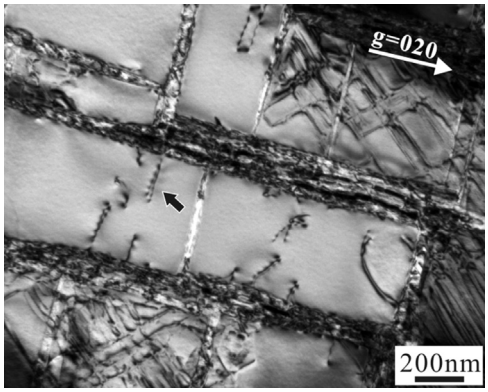

Fig. 6. Bright-field TEM image of the 3Ti alloy deformed in tension at 700 °C to 5%. Beam direction close to the [001] zone axial using a (020) reflection.

Fig. 8 shows general features of the dislocation substructures observed in the 3Ti alloy after deformation at 800 °C. A typical feature is dislocations shearing into the γ′ precipitates (marked by black arrow). SFs extending across the γ′ precipitates are frequently observed. The density of SFs at 800 °C is higher than that at 700 °C and 600 °C. Some SFs are originated from the γ/γ′ interfaces, which is likely due to the dissociation of $a/2\langle 110\rangle$ matrix dislocation at the γ/γ′ interface. The $a/3\langle 112\rangle$ dislocation shears into the γ′ precipitate leaving a SISF behind it, and the $a/6\langle 112\rangle$ remains at the γ/γ′ interface. The SISF energy represents a barrier which prevents the $a/3\langle 112\rangle$ dislocation from shearing into the γ′ precipitate. It is reported that the addition of Ti can improve SISF energy [9]. This may contribute to the improved yield strength at 800 °C.

3.4.2. *The high temperature range (900–1000 °C)*

The dislocation configurations at 900 °C are shown in Fig. 9. Some straight dislocations in the γ′ precipitates are observed (Fig. 9a, marked by black arrows), implying the shearing mechanism.

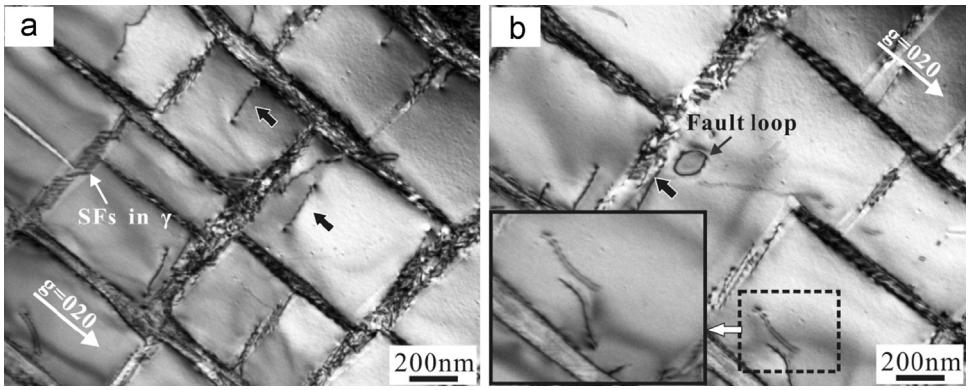

Fig. 5. Bright-field TEM images of the 3Ti alloy deformed to 5% in tension at 600 °C. (a) Pairs of dislocations in the γ′ precipitates and SFs in the γ channels. (b) Pairs of dislocations in the γ′ precipitates and fault loop within the γ′ precipitates. Beam direction close to the [001] zone axial using a (020) reflection.

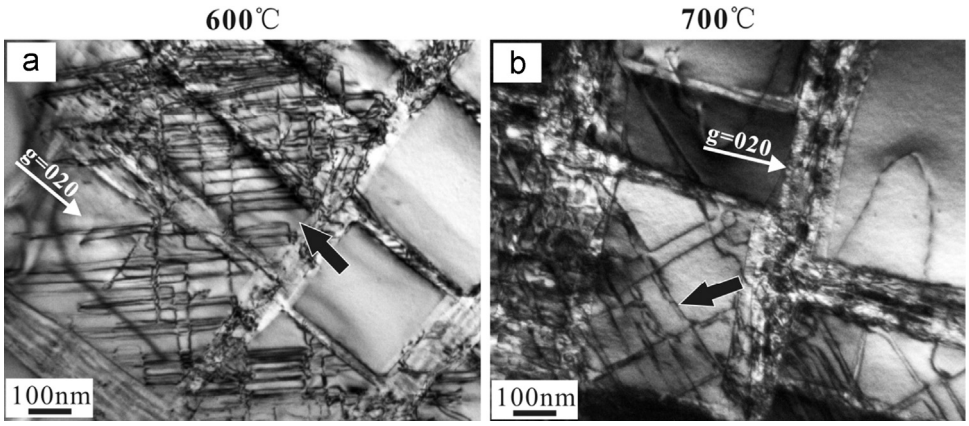

Fig. 7. Bright-field TEM images showing dislocation networks of the 3Ti alloy deformed in tension at (a) 600 °C to 5% and (b) 700 °C to 5%. Beam direction close to the [001] zone axial using a (020) reflection.

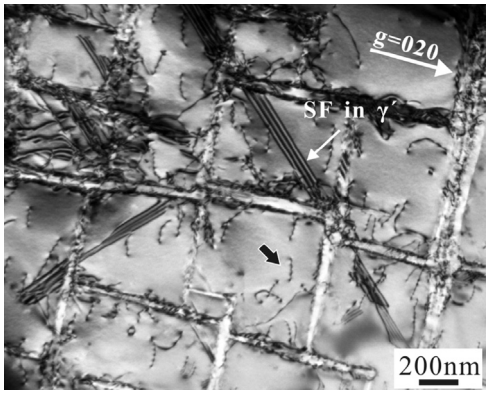

Fig. 8. Bright-field TEM image of the 3Ti alloy deformed in tension at 800 °C to 5%. Beam direction close to the [001] zone axial using a (020) reflection.

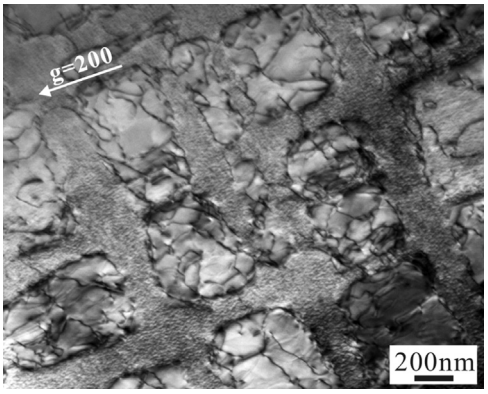

Fig. 10. Bright-field TEM image of the 3Ti alloy deformed in tension at 1000 °C to 5%. Beam direction close to the [001] zone axial using a (200) reflection.

Bypassing of the γ′ particles by dislocations is another dominant feature (Fig. 9b, marked by white arrows). This indicates that the deformation mechanism begins to change from the γ′ shearing to bypassing which is dominated by Orowan looping, and such variation of deformation mode will cause the decrease of the strength.

Fig. 10 shows the configuration of the dislocations after deformation at 1000 °C. In comparison with the γ′ precipitates sheared by dislocations below 900 °C, deformation at 1000 °C is mainly via bypassing of the γ′ particles by dislocations. It can be seen that the channel width is increased and the γ/γ′ interfaces become mellow, indicating that the γ′ precipitates are partially dissolved during the test. The dissolution of the γ′ precipitates is likely due to the high test temperature which is above the annealing temperature (aged at 950 °C). As shown in Fig. 1, increasing the annealing temperature, the volume faction of the γ′ precipitates is decreased. And an applied stress may promote the diffusion of atoms and accelerate the dissolution of the γ′ precipitates

4. Discussion

4.1. Microstructural stability

The theoretical analysis on thermodynamic stability of the Co_3X (X=Al, Ti, W) and Ni_3Al with $L1_2$ structure may provide a

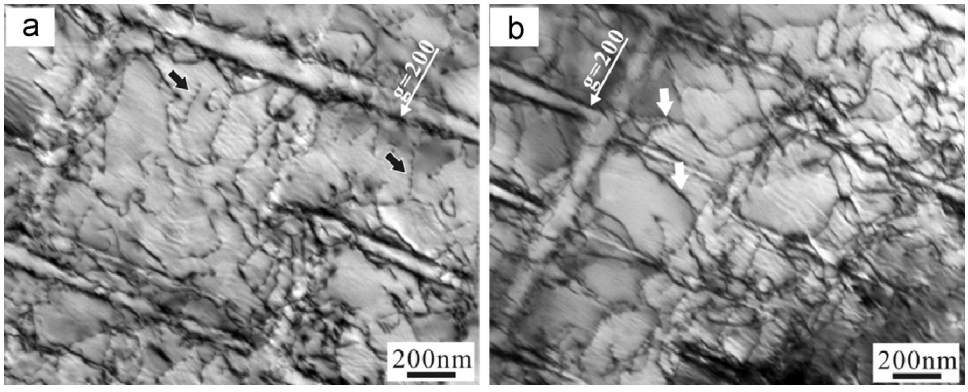

Fig. 9. Bright-field TEM images of the 3Ti alloy deformed in tension at 900 °C to 5%. (a) Dislocations shearing of the γ′ precipitates. (b) Dislocations bypassing of the γ′ precipitates. Beam direction close to the [001] zone axial using a (200) reflection.

better understanding of the improved microstructural stability after alloying. Generally, the formation energy and the bonding energy between atoms can be used to characterize the phase stability of intermetallic compounds. The greater negative formation energy and larger bonding energy implies more stable phase to be formed. Results from Xu et al. [21] show that the $L1_2$ type Ni_3Al and Co_3Ti compounds have a relatively lager negative formation energy, and the bonds between Ni atoms and Al atoms as well as the bonds between Co atoms and Ti atoms are stronger, compared to the Co_3Al and Co_3W with $L1_2$ structure. In the current study, the nominal stoichiometry of the γ′ phase can be deduced as $(Co, Ni)_3(Al, W, Ni, Ti)$ based on the data from EPMA. Most of Ni atoms occupy Co sites and Ti atoms occupy Al/W sites, contributing to the formation of the stronger bonding between Ni atoms and Al atoms as well as between Co atoms and Ti atoms. As a result, a combined addition of Ti and Ni is more effective to improve the γ′-Co_3 (Al,W) stability, despite of the significant decrease of W amount.

4.2. Tensile properties

As shown in Fig.3, from room temperature to 800 °C, the yield strength of the 3Ti alloy is superior compared to the other two single-crystal Co–Al–W-alloys. However, above 800 °C, the yield strength deceases rapidly with temperature increasing. The dislocation microstructures after deformation at various temperatures show that the major deformation mechanism from room temperature to 800 °C is dislocations shearing of the γ′ precipitates by pairs of $a/2\langle 110\rangle$-type dislocations and above 800 °C dislocations bypassing the γ′ precipitates becomes the main mode.

It has been confirmed that a $a/2\langle 110\rangle$-type dislocation traveling in the γ matrix cannot enter the γ′ precipitates without the formation of an anti-phase boundary (APB), and therefore pairs of $a/2\langle 110\rangle$-type dislocations shear the γ′ precipitates, with a second $a/2\langle 110\rangle$-type dislocation removing the APB introduced by the first [1]. The associated APB energy, γ_{APB}, represents a barrier which must be overcome if the cutting of particle occurs, and the precipitate-cutting stress is expected to be in the order γ_{APB}/b, where b is the Burgers vector. Recent results by Titus [22] suggest that the APB energy can be decreased greatly with large amount of Ni additions (29–38 at%) in Co–Al–W-base alloys, and the APB energy of the Ni-containing Co–Al–W-base alloys at 900 °C is only one fifth of the value in ternary Co–Al–W-base alloys. In the present study, the Ni content is about 17 at%, much lower than the value reported in Ref. [22], suggesting the decrease of APB energy in the 3Ti alloy is not as serious as these reported Ni-containing Co–Al–W-base alloys [22]. The APB energy of the $Co_3(Al,W)$ compound is not sensitive to temperature from R.T. to 700 °C [23]. The size and volume faction of the γ′ precipitates of the 3Ti alloy is much similar with that of the single-crystal Co–8.8Al–9.8W–2Ta (at%) [7]. The yield strength of the 3Ti alloy below 800 °C is supposed to be lower than that of the Co–8.8Al–9.8W–2Ta (at%), which is contrary with the experiment results in the present study. So far, the effect of Ti additions on the APB energy of the $Co_3(Al,W)$ compound is not clear. In view of the improvement of yield strength, it can be inferred that the addition of Ti increases the APB energy of the Co_3 (Al,W).

In the high-temperature range (900–1000 °C), the major defects are dislocations bypassing the γ′ precipitates. Before the dislocations can spread in the matrix, the applied stress must be high enough to overcome the local Orowan resistance of the channels, which is simply

$$\tau = \sqrt{\frac{2}{3}}\frac{Gb}{h}$$

where G is the shear modulus, b the Burgers vector, and h is the channel width. For the 3Ti alloy, due to the partial dissolution of the γ′ precipitates, the channel width is much larger than that of the Co–8.8Al–9.8W–2Ta (at%) and the Co–10Al–5W–17Ni–6Cr–2.7Ta (at%) [7,16], suggesting a lower dislocation resistance. Therefore, increasing the γ′ volume fraction and decreasing the channel width will improve the high-temperature strength. This can be realized by further additions of alloying γ′-forming elements such as Ti and appropriate heat treatments. On the other hand, the level of mobility of the matrix dislocations is also dependent on the intrinsic strength of the γ matrix. In the present alloy, the equilibrium content of W in the γ matrix at 1000 °C is about 3.34 at% (~10 wt%). For the Co–10Al–10W (at%), the equilibrium content of W in the γ matrix at 900 °C is about 7.7 at% (~16 wt%) [13]. As shown in Fig. 3, the yield stress of 3Ti and the Co–9.4Al–10.7W (at%) decrease rapidly above 900 °C. This indicates that a high amount of W in the γ matrix is not effective to impede the motion of dislocations in channels. Alloying Re in Ni-base alloys assists in improving the intrinsic strength of the γ matrix by reducing the interdiffusion coefficients and the climb velocity of dislocations in the γ phases [24]. In Ref. [7], the yield strength of a Re-containing polycrystalline Co–Al–W-base alloy is much lower than that of Re-free polycrystalline Co–Al–W-base alloys, which is attributed to the formation of a γ+Co_3W two-phase layer along the grain boundary. The amount of W in the 3Ti alloy is about 5 at%, much lower compared to the Co–Al–W-base alloys reported in Ref. [7]. This indicates that the addition of Re may not contribute to the formation of Co_3W and could harden Ni-containing Co–Al–W-base alloys. In the future work, it is necessary to seek elements that can increase the intrinsic strength of the γ matrix and reduce the climb velocity of dislocations, which will increase the resistance of dislocation motion and improve high-temperature strength of Co–Al–W-base superalloys.

5. Conclusions

The microstructure stability and tensile properties of a Ti-containing single-crystal Co–Al–W-base superalloy have been characterized. The following conclusions can be drawn:

1. Despite of the great reduction of tungsten amount, the alloy still possesses a relatively higher γ′ solvus temperature with a combined addition of Ni and Ti. After aging at 900–1000 °C for 400 h, the 3Ti alloy still exhibits the γ–γ′ microstructure without the presence of secondary phases, suggesting its relatively stable microstructure at high temperature.
2. From room temperature to 800 °C, the tensile strength of the 3Ti alloy is superior compared to those single-crystal Co–Al–W-base alloys. However, above 800 °C, the yield stress decreases rapidly with temperature increasing. The major deformation mechanisms of the 3Ti alloy consist of shearing of the γ′ precipitates by pairs of $a/2\langle 110\rangle$-type dislocations from room temperature to 800 °C and bypassing of the γ′ precipitates by unpaired $a/2\langle 110\rangle$-type dislocation dislocations above 900 °C. At 900 °C, it shows a transition from the γ′ shearing to bypassing.

Acknowledgment

This work was partly supported by the High Technology Research and Development Program of China (No. 2014AA041701) and the National Natural Science Foundation of China (NFSC) under Grant nos. 51171179, 51271174, 51331005, and 11332010.

References

[1] R.C. Reed, The Superalloys: Fundamentals and Applications, Cambridge Press, New York, 2006.
[2] J. Sato, T. Omori, K. Oikawa, I. Ohnuma, R. Kainuma, K. Ishida, Science 312 (2006) 90.
[3] A. Bauera, S. Neumeiera, F. Pyczak, R.F. Singer, M. Göken, Mater. Sci. Eng. A 550 (2012) 333.
[4] S. Kobayashi, Y. Tsukamoto, T. Takasugi, Intermetallics 19 (2011) 1908.
[5] C.H. Zenk, S. Neumeier, H.J. Stone, M. Göken, Intermetallics 55 (2014) 28.
[6] A. Suzuki, G.C. DeNolf, T.M. Pollock, Scr. Mater. 56 (2007) 385.
[7] A. Suzuki, T.M. Pollock, Acta Mater. 56 (2008) 1288.
[8] F. Xue, H.J. Zhou, Q. Feng, J. Mater. 66 (2014) 2486.
[9] A. Mottura, A. Janotti, T.M. Pollock, Intermetallics 28 (2012) 138.
[10] M.S. Titus, Y.M. Eggeler, A. Suzuki, T.M. Pollock, Acta Mater. 82 (2015) 530.
[11] K. Shinagawa, T. Omori, J. Sato, K. Oikawa, I. Ohnuma, R. Kainuma, K. Ishida1, Mater. Trans. 49 (2008) 1474.
[12] H.-Y. Yan, V.A. Vorontsov, D. Dye, Intermetallics 48 (2014) 44.
[13] T. Omori, K. Oikawa, J. Sato, I. Ohnuma, U.R. Kattner, R. Kainuma, K. Ishida, Intermetallics 32 (2013) 274.
[14] S. Meher, H.-Y. Yan, S. Nag, D. Dye, R. Banerjee, Scr. Mater. 67 (2012) 850.
[15] I. Povstugar, Pyuck-Pa Choi, S. Neumeier, A. Bauer, C.H. Zenk, M. Göken, D. Raabe, Acta Mater. 78 (2014) 78.
[16] L. Shi, J.J. Yu, C.Y. Cui, X.F. Sun, Mater. Sci. Eng. A 620 (2014) 36.
[17] B. Décamps, S. Raujol, A. Coujou, F. Pettinari-Sturmel, N. Clément, D. Locq, P. Caron, Philos. Mag. A 84 (2004) 91.
[18] F. Pyczak, A. Bauer, M. Göken, S. Neumeier, U. Lorenz, M. Oehring, N. Schell, A. Schreyer, A. Stark, F. Symanzik, Mater. Sci. Eng. A 571 (2013) 13.
[19] F. Diologent, P. Caron, Mater. Sci. Eng. A 385 (2004) 245.
[20] T.M. Pollock, A.S. Argon, Acta Metall. Mater. 40 (1992) 1.
[21] W.W. Xu, J.J. Han, Z.W. Wang, C.P. Wang, Y.H. Wen, X.J. Liua, Z.Z. Zhu, Intermetallics 32 (2013) 303.
[22] M.S. Titus, A. Mottura, G.B. Viswanathan, A. Suzuki, M.J. Mills, T.M. Pollock, Acta Mater. 89 (2015) 423.
[23] N.L. Okamoto, T. Oohashi, H. Adachi, K. Kishida, H. Inui, P. Veyssière, Philos. Mag. 91 (2011) 3667.
[24] L.J. Carroll, Q. Feng, T.M. Pollock, Metall. Mater. Trans. A 39 (2008) 1290.